

Search for Higgs Bosons Decaying to Tau Pairs in $p\bar{p}$ Collisions with the D0 Detector

V. M. Abazov,³⁶ B. Abbott,⁷⁵ M. Abolins,⁶⁵ B. S. Acharya,²⁹ M. Adams,⁵¹ T. Adams,⁴⁹ E. Aguilo,⁶ S. H. Ahn,³¹ M. Ahsan,⁵⁹ G. D. Alexeev,³⁶ G. Alkhalaf,⁴⁰ A. Alton,^{64,*} G. Alverson,⁶³ G. A. Alves,² M. Anastasoae,³⁵ L. S. Ancu,³⁵ T. Andeen,⁵³ S. Anderson,⁴⁵ B. Andrieu,¹⁷ M. S. Anzels,⁵³ M. Aoki,⁵⁰ Y. Arnoud,¹⁴ M. Arov,⁶⁰ M. Arthaud,¹⁸ A. Askew,⁴⁹ B. Åsman,⁴¹ A. C. S. Assis Jesus,³ O. Atramentov,⁴⁹ C. Avila,⁸ F. Badaud,¹³ A. Baden,⁶¹ L. Bagby,⁵⁰ B. Baldin,⁵⁰ D. V. Bandurin,⁵⁹ P. Banerjee,²⁹ S. Banerjee,²⁹ E. Barberis,⁶³ A.-F. Barfuss,¹⁵ P. Bargassa,⁸⁰ P. Baringer,⁵⁸ J. Barreto,² J. F. Bartlett,⁵⁰ U. Bassler,¹⁸ D. Bauer,⁴³ S. Beale,⁶ A. Bean,⁵⁸ M. Begalli,³ M. Begel,⁷³ C. Belanger-Champagne,⁴¹ L. Bellantoni,⁵⁰ A. Bellavance,⁵⁰ J. A. Benitez,⁶⁵ S. B. Beri,²⁷ G. Bernardi,¹⁷ R. Bernhard,²³ I. Bertram,⁴² M. Besançon,¹⁸ R. Beuselinck,⁴³ V. A. Bezzubov,³⁹ P. C. Bhat,⁵⁰ V. Bhatnagar,²⁷ C. Biscarat,²⁰ G. Blazey,⁵² F. Blekman,⁴³ S. Blessing,⁴⁹ D. Bloch,¹⁹ K. Bloom,⁶⁷ A. Boehnlein,⁵⁰ D. Boline,⁶² T. A. Bolton,⁵⁹ E. E. Boos,³⁸ G. Borissov,⁴² T. Bose,⁷⁷ A. Brandt,⁷⁸ R. Brock,⁶⁵ G. Brooijmans,⁷⁰ A. Bross,⁵⁰ D. Brown,⁸¹ N. J. Buchanan,⁴⁹ D. Buchholz,⁵³ M. Buehler,⁸¹ V. Buescher,²² V. Bunichev,³⁸ S. Burdin,^{42,†} S. Burke,⁴⁵ T. H. Burnett,⁸² C. P. Buszello,⁴³ J. M. Butler,⁶² P. Calfayan,²⁵ S. Calvet,¹⁶ J. Cammin,⁷¹ W. Carvalho,³ B. C. K. Casey,⁵⁰ H. Castilla-Valdez,³³ S. Chakrabarti,¹⁸ D. Chakraborty,⁵² K. Chan,⁶ K. M. Chan,⁵⁵ A. Chandra,⁴⁸ F. Charles,^{19,**} E. Cheu,⁴⁵ F. Chevallier,¹⁴ D. K. Cho,⁶² S. Choi,³² B. Choudhary,²⁸ L. Christofek,⁷⁷ T. Christoudias,⁴³ S. Cihangir,⁵⁰ D. Claes,⁶⁷ J. Clutter,⁵⁸ M. Cooke,⁸⁰ W. E. Cooper,⁵⁰ M. Corcoran,⁸⁰ F. Couderc,¹⁸ M.-C. Cousinou,¹⁵ S. Crépe-Renaudin,¹⁴ D. Cutts,⁷⁷ M. Ćwiok,³⁰ H. da Motta,² A. Das,⁴⁵ G. Davies,⁴³ K. De,⁷⁸ S. J. de Jong,³⁵ E. De La Cruz-Burelo,⁶⁴ C. De Oliveira Martins,³ J. D. Degenhardt,⁶⁴ F. Déliot,¹⁸ M. Demarteau,⁵⁰ R. Demina,⁷¹ D. Denisov,⁵⁰ S. P. Denisov,³⁹ S. Desai,⁵⁰ H. T. Diehl,⁵⁰ M. Diesburg,⁵⁰ A. Dominguez,⁶⁷ H. Dong,⁷² L. V. Dudko,³⁸ L. Duflo,¹⁶ S. R. Dugad,²⁹ D. Duggan,⁴⁹ A. Duperrin,¹⁵ J. Dyer,⁶⁵ A. Dyshkant,⁵² M. Eads,⁶⁷ D. Edmunds,⁶⁵ J. Ellison,⁴⁸ V. D. Elvira,⁵⁰ Y. Enari,⁷⁷ S. Eno,⁶¹ P. Ermolov,³⁸ H. Evans,⁵⁴ A. Evdokimov,⁷³ V. N. Evdokimov,³⁹ A. V. Ferapontov,⁵⁹ T. Ferbel,⁷¹ F. Fiedler,²⁴ F. Filthaut,³⁵ W. Fisher,⁵⁰ H. E. Fisk,⁵⁰ M. Fortner,⁵² H. Fox,⁴² S. Fu,⁵⁰ S. Fuess,⁵⁰ T. Gadfort,⁷⁰ C. F. Galea,³⁵ E. Gallas,⁵⁰ C. Garcia,⁷¹ A. Garcia-Bellido,⁸² V. Gavrilov,³⁷ P. Gay,¹³ W. Geist,¹⁹ D. Gelé,¹⁹ C. E. Gerber,⁵¹ Y. Gershtein,⁴⁹ D. Gillberg,⁶ G. Ginther,⁷¹ N. Gollub,⁴¹ B. Gómez,⁸ A. Goussiou,⁸² P. D. Grannis,⁷² H. Greenlee,⁵⁰ Z. D. Greenwood,⁶⁰ E. M. Gregores,⁴ G. Grenier,²⁰ Ph. Gris,¹³ J.-F. Grivaz,¹⁶ A. Grohsjean,²⁵ S. Grünendahl,⁵⁰ M. W. Grünewald,³⁰ F. Guo,⁷² J. Guo,⁷² G. Gutierrez,⁵⁰ P. Gutierrez,⁷⁵ A. Haas,⁷⁰ N. J. Hadley,⁶¹ P. Haefner,²⁵ S. Hagopian,⁴⁹ J. Haley,⁶⁸ I. Hall,⁶⁵ R. E. Hall,⁴⁷ L. Han,⁷ K. Harder,⁴⁴ A. Harel,⁷¹ J. M. Hauptman,⁵⁷ R. Hauser,⁶⁵ J. Hays,⁴³ T. Hebbeker,²¹ D. Hedin,⁵² J. G. Hegeman,³⁴ A. P. Heinson,⁴⁸ U. Heintz,⁶² C. Hensel,^{22,§} K. Herner,⁷² G. Hesketh,⁶³ M. D. Hildreth,⁵⁵ R. Hirosky,⁸¹ J. D. Hobbs,⁷² B. Hoeneisen,¹² H. Hoeth,²⁶ M. Hohlfield,²² S. J. Hong,³¹ S. Hossain,⁷⁵ P. Houben,³⁴ Y. Hu,⁷² Z. Hubacek,¹⁰ V. Hynek,⁹ I. Iashvili,⁶⁹ R. Illingworth,⁵⁰ A. S. Ito,⁵⁰ S. Jabeen,⁶² M. Jaffré,¹⁶ S. Jain,⁷⁵ K. Jakobs,²³ C. Jarvis,⁶¹ R. Jesik,⁴³ K. Johns,⁴⁵ C. Johnson,⁷⁰ M. Johnson,⁵⁰ A. Jonckheere,⁵⁰ P. Jonsson,⁴³ A. Juste,⁵⁰ E. Kajfasz,¹⁵ J. M. Kalk,⁶⁰ D. Karmanov,³⁸ P. A. Kasper,⁵⁰ I. Katsanos,⁷⁰ D. Kau,⁴⁹ V. Kaushik,⁷⁸ R. Kehoe,⁷⁹ S. Kermiche,¹⁵ N. Khalatyan,⁵⁰ A. Khanov,⁷⁶ A. Kharchilava,⁶⁹ Y. M. Kharzheev,³⁶ D. Khatidze,⁷⁰ T. J. Kim,³¹ M. H. Kirby,⁵³ M. Kirsch,²¹ B. Klima,⁵⁰ J. M. Kohli,²⁷ J.-P. Konrath,²³ A. V. Kozelov,³⁹ J. Kraus,⁶⁵ D. Krop,⁵⁴ T. Kuhl,²⁴ A. Kumar,⁶⁹ A. Kupco,¹¹ T. Kurča,²⁰ V. A. Kuzmin,³⁸ J. Kvita,⁹ F. Lacroix,¹³ D. Lam,⁵⁵ S. Lammers,⁷⁰ G. Landsberg,⁷⁷ P. Lebrun,²⁰ W. M. Lee,⁵⁰ A. Leflat,³⁸ J. Lellouch,¹⁷ J. Leveque,⁴⁵ J. Li,⁷⁸ L. Li,⁴⁸ Q. Z. Li,⁵⁰ S. M. Lietti,⁵ J. G. R. Lima,⁵² D. Lincoln,⁵⁰ J. Linnemann,⁶⁵ V. V. Lipaev,³⁹ R. Lipton,⁵⁰ Y. Liu,⁷ Z. Liu,⁶ A. Lobodenko,⁴⁰ M. Lokajicek,¹¹ P. Love,⁴² H. J. Lubatti,⁸² R. Luna,³ A. L. Lyon,⁵⁰ A. K. A. Maciel,² D. Mackin,⁸⁰ R. J. Madaras,⁴⁶ P. Mättig,²⁶ C. Magass,²¹ A. Magerkurth,⁶⁴ P. K. Mal,⁸² H. B. Malbouisson,³ S. Malik,⁶⁷ V. L. Malyshev,³⁶ H. S. Mao,⁵⁰ Y. Maravin,⁵⁹ B. Martin,¹⁴ R. McCarthy,⁷² A. Melnitchouk,⁶⁶ L. Mendoza,⁸ P. G. Mercadante,⁵ M. Merkin,³⁸ K. W. Merritt,⁵⁰ A. Meyer,²¹ J. Meyer,^{22,§} T. Millet,²⁰ J. Mitrevski,⁷⁰ R. K. Mommsen,⁴⁴ N. K. Mondal,²⁹ R. W. Moore,⁶ T. Moulik,⁵⁸ G. S. Muanza,²⁰ M. Mulhearn,⁷⁰ O. Mundal,²² L. Mundim,³ E. Nagy,¹⁵ M. Naimuddin,⁵⁰ M. Narain,⁷⁷ N. A. Naumann,³⁵ H. A. Neal,⁶⁴ J. P. Negret,⁸ P. Neustroev,⁴⁰ H. Nilsen,²³ H. Nogima,³ S. F. Novaes,⁵ T. Nunnemann,²⁵ V. O'Dell,⁵⁰ D. C. O'Neil,⁶ G. Obrant,⁴⁰ C. Ochando,¹⁶ D. Onoprienko,⁵⁹ N. Oshima,⁵⁰ N. Osman,⁴³ J. Osta,⁵⁵ R. Otec,¹⁰ G. J. Otero y Garzón,⁵⁰ M. Owen,⁴⁴ P. Padley,⁸⁰ M. Pangilinan,⁷⁷ N. Parashar,⁵⁶ S.-J. Park,^{22,§} S. K. Park,³¹ J. Parsons,⁷⁰ R. Partridge,⁷⁷ N. Parua,⁵⁴ A. Patwa,⁷³ G. Pawloski,⁸⁰ B. Penning,²³ M. Perfilov,³⁸ K. Peters,⁴⁴ Y. Peters,²⁶ P. Pétroff,¹⁶ M. Petteni,⁴³ R. Piegaia,¹ J. Piper,⁶⁵ M.-A. Pleier,²² P. L. M. Podesta-Lerma,^{33,‡} V. M. Podstavkov,⁵⁰ Y. Pogorelov,⁵⁵ M.-E. Pol,² P. Polozov,³⁷ B. G. Pope,⁶⁵ A. V. Popov,³⁹ C. Potter,⁶ W. L. Prado da Silva,³ H. B. Prosper,⁴⁹ S. Protopopescu,⁷³ J. Qian,⁶⁴ A. Quadt,^{22,§} B. Quinn,⁶⁶ A. Rakitine,⁴² M. S. Rangel,² K. Ranjan,²⁸ P. N. Ratoff,⁴² P. Renkel,⁷⁹ S. Reucroft,⁶³ P. Rich,⁴⁴ J. Rieger,⁵⁴ M. Rijssenbeek,⁷² I. Ripp-Baudot,¹⁹ F. Rizatdinova,⁷⁶ S. Robinson,⁴³ R. F. Rodrigues,³

M. Rominsky,⁷⁵ C. Royon,¹⁸ P. Rubinov,⁵⁰ R. Ruchti,⁵⁵ G. Safronov,³⁷ G. Sajot,¹⁴ A. Sánchez-Hernández,³³ M. P. Sanders,¹⁷ B. Sanghi,⁵⁰ A. Santoro,³ G. Savage,⁵⁰ L. Sawyer,⁶⁰ T. Scanlon,⁴³ D. Schaile,²⁵ R. D. Schamberger,⁷² Y. Scheglov,⁴⁰ H. Schellman,⁵³ T. Schliephake,²⁶ C. Schwanenberger,⁴⁴ A. Schwartzman,⁶⁸ R. Schwienhorst,⁶⁵ J. Sekaric,⁴⁹ H. Severini,⁷⁵ E. Shabalina,⁵¹ M. Shamim,⁵⁹ V. Shary,¹⁸ A. A. Shchukin,³⁹ R. K. Shivpuri,²⁸ V. Siccaldi,¹⁹ V. Simak,¹⁰ V. Sirotenko,⁵⁰ P. Skubic,⁷⁵ P. Slattery,⁷¹ D. Smirnov,⁵⁵ G. R. Snow,⁶⁷ J. Snow,⁷⁴ S. Snyder,⁷³ S. Söldner-Rembold,⁴⁴ L. Sonnenschein,¹⁷ A. Sopczak,⁴² M. Sosebee,⁷⁸ K. Soustruznik,⁹ B. Spurlock,⁷⁸ J. Stark,¹⁴ J. Steele,⁶⁰ V. Stolin,³⁷ D. A. Stoyanova,³⁹ J. Strandberg,⁶⁴ S. Strandberg,⁴¹ M. A. Strang,⁶⁹ E. Strauss,⁷² M. Strauss,⁷⁵ R. Ströhmer,²⁵ D. Strom,⁵³ L. Stutte,⁵⁰ S. Sumowidagdo,⁴⁹ P. Svoisky,⁵⁵ A. Sznajder,³ P. Tamburello,⁴⁵ A. Tanasijczuk,¹ W. Taylor,⁶ J. Temple,⁴⁵ B. Tiller,²⁵ F. Tissandier,¹³ M. Titov,¹⁸ V. V. Tokmenin,³⁶ T. Toole,⁶¹ I. Torchiani,²³ T. Trefzger,²⁴ D. Tsybychev,⁷² B. Tuchming,¹⁸ C. Tully,⁶⁸ P. M. Tuts,⁷⁰ R. Unalan,⁶⁵ L. Uvarov,⁴⁰ S. Uvarov,⁴⁰ S. Uzunyan,⁵² B. Vachon,⁶ P. J. van den Berg,³⁴ R. Van Kooten,⁵⁴ W. M. van Leeuwen,³⁴ N. Varelas,⁵¹ E. W. Varnes,⁴⁵ I. A. Vasilyev,³⁹ M. Vaupel,²⁶ P. Verdier,²⁰ L. S. Vertogradov,³⁶ M. Verzocchi,⁵⁰ F. Villeneuve-Seguiier,⁴³ P. Vint,⁴³ P. Vokac,¹⁰ E. Von Toerne,⁵⁹ M. Voutilainen,^{68,||} R. Wagner,⁶⁸ H. D. Wahl,⁴⁹ L. Wang,⁶¹ M. H. L. S. Wang,⁵⁰ J. Warchol,⁵⁵ G. Watts,⁸² M. Wayne,⁵⁵ G. Weber,²⁴ M. Weber,⁵⁰ L. Welty-Rieger,⁵⁴ A. Wenger,^{23,¶} N. Wermes,²² M. Wetstein,⁶¹ A. White,⁷⁸ D. Wicke,²⁶ G. W. Wilson,⁵⁸ S. J. Wimpenny,⁴⁸ M. Wobisch,⁶⁰ D. R. Wood,⁶³ T. R. Wyatt,⁴⁴ Y. Xie,⁷⁷ S. Yacoob,⁵³ R. Yamada,⁵⁰ M. Yan,⁶¹ W.-C. Yang,⁴⁴ T. Yasuda,⁵⁰ Y. A. Yatsunenko,³⁶ K. Yip,⁷³ H. D. Yoo,⁷⁷ S. W. Youn,⁵³ J. Yu,⁷⁸ C. Zeitnitz,²⁶ T. Zhao,⁸² B. Zhou,⁶⁴ J. Zhu,⁷² M. Zielinski,⁷¹ D. Zieminska,⁵⁴ A. Zieminski,^{54,**} L. Zivkovic,⁷⁰ V. Zutshi,⁵² and E. G. Zverev³⁸

(The D0 Collaboration)

¹Universidad de Buenos Aires, Buenos Aires, Argentina

²LAFEX, Centro Brasileiro de Pesquisas Físicas, Rio de Janeiro, Brazil

³Universidade do Estado do Rio de Janeiro, Rio de Janeiro, Brazil

⁴Universidade Federal do ABC, Santo André, Brazil

⁵Instituto de Física Teórica, Universidade Estadual Paulista, São Paulo, Brazil

⁶University of Alberta, Edmonton, Alberta, Canada,

Simon Fraser University, Burnaby, British Columbia, Canada,

York University, Toronto, Ontario, Canada,

and McGill University, Montreal, Quebec, Canada

⁷University of Science and Technology of China, Hefei, People's Republic of China

⁸Universidad de los Andes, Bogotá, Colombia

⁹Center for Particle Physics, Charles University, Prague, Czech Republic

¹⁰Czech Technical University, Prague, Czech Republic

¹¹Center for Particle Physics, Institute of Physics, Academy of Sciences of the Czech Republic, Prague, Czech Republic

¹²Universidad San Francisco de Quito, Quito, Ecuador

¹³LPC, Univ Blaise Pascal, CNRS/IN2P3, Clermont, France

¹⁴LPSC, Université Joseph Fourier Grenoble 1, CNRS/IN2P3, Institut National Polytechnique de Grenoble, France

¹⁵CPPM, Aix-Marseille Université, CNRS/IN2P3, Marseille, France

¹⁶LAL, Univ Paris-Sud, IN2P3/CNRS, Orsay, France

¹⁷LPNHE, IN2P3/CNRS, Universités Paris VI and VII, Paris, France

¹⁸DAPNIA/Service de Physique des Particules, CEA, Saclay, France

¹⁹IPHC, Université Louis Pasteur et Université de Haute Alsace, CNRS/IN2P3, Strasbourg, France

²⁰IPNL, Université Lyon 1, CNRS/IN2P3, Villeurbanne, France and Université de Lyon, Lyon, France

²¹III. Physikalisches Institut A, RWTH Aachen, Aachen, Germany

²²Physikalisches Institut, Universität Bonn, Bonn, Germany

²³Physikalisches Institut, Universität Freiburg, Freiburg, Germany

²⁴Institut für Physik, Universität Mainz, Mainz, Germany

²⁵Ludwig-Maximilians-Universität München, München, Germany

²⁶Fachbereich Physik, University of Wuppertal, Wuppertal, Germany

²⁷Panjab University, Chandigarh, India

²⁸Delhi University, Delhi, India

²⁹Tata Institute of Fundamental Research, Mumbai, India

³⁰University College Dublin, Dublin, Ireland

³¹Korea Detector Laboratory, Korea University, Seoul, Korea

³²SungKyunKwan University, Suwon, Korea

³³CINVESTAV, Mexico City, Mexico

- ³⁴*FOM-Institute NIKHEF and University of Amsterdam/NIKHEF, Amsterdam, The Netherlands*
³⁵*Radboud University Nijmegen/NIKHEF, Nijmegen, The Netherlands*
³⁶*Joint Institute for Nuclear Research, Dubna, Russia*
³⁷*Institute for Theoretical and Experimental Physics, Moscow, Russia*
³⁸*Moscow State University, Moscow, Russia*
³⁹*Institute for High Energy Physics, Protvino, Russia*
⁴⁰*Petersburg Nuclear Physics Institute, St. Petersburg, Russia*
⁴¹*Lund University, Lund, Sweden, Royal Institute of Technology and Stockholm University, Stockholm, Sweden, and Uppsala University, Uppsala, Sweden*
⁴²*Lancaster University, Lancaster, United Kingdom*
⁴³*Imperial College, London, United Kingdom*
⁴⁴*University of Manchester, Manchester, United Kingdom*
⁴⁵*University of Arizona, Tucson, Arizona 85721, USA*
⁴⁶*Lawrence Berkeley National Laboratory and University of California, Berkeley, California 94720, USA*
⁴⁷*California State University, Fresno, California 93740, USA*
⁴⁸*University of California, Riverside, California 92521, USA*
⁴⁹*Florida State University, Tallahassee, Florida 32306, USA*
⁵⁰*Fermi National Accelerator Laboratory, Batavia, Illinois 60510, USA*
⁵¹*University of Illinois at Chicago, Chicago, Illinois 60607, USA*
⁵²*Northern Illinois University, DeKalb, Illinois 60115, USA*
⁵³*Northwestern University, Evanston, Illinois 60208, USA*
⁵⁴*Indiana University, Bloomington, Indiana 47405, USA*
⁵⁵*University of Notre Dame, Notre Dame, Indiana 46556, USA*
⁵⁶*Purdue University Calumet, Hammond, Indiana 46323, USA*
⁵⁷*Iowa State University, Ames, Iowa 50011, USA*
⁵⁸*University of Kansas, Lawrence, Kansas 66045, USA*
⁵⁹*Kansas State University, Manhattan, Kansas 66506, USA*
⁶⁰*Louisiana Tech University, Ruston, Louisiana 71272, USA*
⁶¹*University of Maryland, College Park, Maryland 20742, USA*
⁶²*Boston University, Boston, Massachusetts 02215, USA*
⁶³*Northeastern University, Boston, Massachusetts 02115, USA*
⁶⁴*University of Michigan, Ann Arbor, Michigan 48109, USA*
⁶⁵*Michigan State University, East Lansing, Michigan 48824, USA*
⁶⁶*University of Mississippi, University, Mississippi 38677, USA*
⁶⁷*University of Nebraska, Lincoln, Nebraska 68588, USA*
⁶⁸*Princeton University, Princeton, New Jersey 08544, USA*
⁶⁹*State University of New York, Buffalo, New York 14260, USA*
⁷⁰*Columbia University, New York, New York 10027, USA*
⁷¹*University of Rochester, Rochester, New York 14627, USA*
⁷²*State University of New York, Stony Brook, New York 11794, USA*
⁷³*Brookhaven National Laboratory, Upton, New York 11973, USA*
⁷⁴*Langston University, Langston, Oklahoma 73050, USA*
⁷⁵*University of Oklahoma, Norman, Oklahoma 73019, USA*
⁷⁶*Oklahoma State University, Stillwater, Oklahoma 74078, USA*
⁷⁷*Brown University, Providence, Rhode Island 02912, USA*
⁷⁸*University of Texas, Arlington, Texas 76019, USA*
⁷⁹*Southern Methodist University, Dallas, Texas 75275, USA*
⁸⁰*Rice University, Houston, Texas 77005, USA*
⁸¹*University of Virginia, Charlottesville, Virginia 22901, USA*
⁸²*University of Washington, Seattle, Washington 98195, USA*
(Received 16 May 2008; published 14 August 2008)

We present a search for the production of neutral Higgs bosons ϕ decaying into $\tau^+\tau^-$ final states in $p\bar{p}$ collisions at a center-of-mass energy of 1.96 TeV. The data, corresponding to an integrated luminosity of approximately 1 fb^{-1} , were collected by the D0 experiment at the Fermilab Tevatron Collider. Limits on the production cross section times branching ratio are set. The results are interpreted in the minimal supersymmetric standard model yielding limits that are the most stringent to date at hadron colliders.

Higgs bosons are an essential ingredient of electroweak symmetry breaking in the standard model (SM). A search for Higgs bosons (denoted as ϕ) decaying to tau leptons is of particular interest in models with more than one Higgs doublet, where production rates for $p\bar{p} \rightarrow \phi \rightarrow \tau^+\tau^-$ can potentially be large enough for observation at the Fermilab Tevatron Collider. This situation is realized in the minimal supersymmetric standard model (MSSM) [1], which contains two complex Higgs doublets, leading to two neutral CP -even (h, H), one CP -odd (A), and a pair of charged (H^\pm) Higgs bosons. At tree level, the Higgs sector of the MSSM is fully specified by two parameters, generally chosen to be M_A , the mass of the CP -odd Higgs boson, and $\tan\beta$, the ratio of the vacuum expectation values of the two Higgs doublets. Dependence on other MSSM parameters enters through radiative corrections. At large $\tan\beta$, the coupling of the neutral Higgs bosons to down-type quarks and charged leptons is strongly enhanced, leading to sizable cross sections. The Higgs bosons will decay predominantly into third generation fermions.

Searches for neutral MSSM Higgs bosons have been conducted at the CERN LEP collider [2] and at the Tevatron [3–5]. These Tevatron searches used between 260 pb^{-1} and 350 pb^{-1} of collider data. In this Letter a search for $\phi \rightarrow \tau^+\tau^-$ with about 1 fb^{-1} [6] of data is presented. At least one of the tau leptons is required to decay leptonically, leading to final states containing $e\tau_h$, $\mu\tau_h$, and $e\mu$, where τ_h represents a hadronically decaying tau lepton. The data were collected at the Tevatron with the D0 detector between 2002 and 2006 at a $p\bar{p}$ center-of-mass energy $\sqrt{s} = 1.96 \text{ TeV}$. A description of the D0 detector can be found in Ref. [7].

Signal and SM background processes are modeled using the PYTHIA 6.329 [8] Monte Carlo (MC) generator, followed by a GEANT-based [9] simulation of the D0 detector. The signal events are produced with the width of the SM Higgs boson. All background processes, apart from multijet production and W boson production, are normalized using cross sections calculated at next-to-leading order (NLO) and next-to-NLO (for Z boson and Drell-Yan production) based on the CTEQ6.1 [10] parton distribution functions (PDF).

The normalization and shape of background contributions from multijet production, where jets are misidentified as leptons, are estimated from the data by using same charge e and τ_h candidate events ($e\tau_h$ channel) or by selecting background samples by inverting lepton identification criteria ($\mu\tau_h$ and $e\mu$ channels). These samples are normalized to the data at an early stage of the selection in a region of phase space dominated by multijet production. The multijet background estimation in the $\mu\tau_h$ and $e\tau_h$ channels was checked by using an independent method to estimate the background: in the $\mu\tau_h$ channel same charge $\mu\tau_h$ events were used and in the $e\tau_h$ channel the multijet background was estimated from measurements in data of

the probability to misreconstruct electrons from jets. The differences between the estimates were used to set the systematic uncertainty on the multijet production. The normalization of the background from W boson production is obtained from data in a sample dominated by W boson + jet events.

Electrons are selected using their characteristic energy deposits, including the transverse and longitudinal shower profile in the electromagnetic (EM) calorimeter. To reject photons, a reconstructed track is required to point to the energy cluster. Further rejection against background is achieved by using a likelihood discriminant. Muons are selected using reconstructed tracks in the central tracking detector in combination with patterns of hits in the muon detector. Electrons and muons are required to be isolated in the calorimeter and in the case of muons also in the tracker [11]. Events are triggered by inclusive electron and muon triggers. Reconstruction and trigger efficiencies for both leptons are measured in data using $Z/\gamma^* \rightarrow \mu^+\mu^-, e^+e^-$ events.

A hadronically decaying tau lepton is characterized by a narrow isolated jet with low track multiplicity [12]. Three τ -types are distinguished: τ -type 1 is a single track with energy deposited in the hadronic calorimeter (π^\pm -like); τ -type 2 is a single track with energy deposited in the hadronic and the electromagnetic calorimeters (ρ^\pm -like); τ -type 3 is three tracks with an invariant mass below 1.7 GeV , with energy deposited in the calorimeter.

A set of neural networks, NN_τ , one for each τ -type, has been trained to separate hadronic tau decays from jets using $Z/\gamma^* \rightarrow \tau^+\tau^-$ MC events as the signal and multijet data as background. The selections on the neural networks retain 66% of the $Z/\gamma^* \rightarrow \tau^+\tau^-$ events, while rejecting 98% of the multijet background. In addition, a neural network has been trained with electron MC events as background to separate τ -type 2 hadronic tau candidates from electrons (NN_e).

The signal is characterized by two leptons, missing transverse energy \cancel{E}_T and as an enhancement above the background in the visible mass $M_{\text{vis}} = \sqrt{(P_{\tau_1} + P_{\tau_2} + \cancel{P}_T)^2}$, calculated using the four-vectors of the visible tau decay products $P_{\tau_{1,2}}$ and of the missing momentum $\cancel{P}_T = (\cancel{E}_T, \cancel{E}_x, \cancel{E}_y, 0)$. The components \cancel{E}_x and \cancel{E}_y of \cancel{E}_T are computed from calorimeter cells and the momentum of muons, and corrected for the energy response of electrons, taus, and jets. The four-vectors of the hadronic taus are calculated using the calorimeter for τ -types 2 and 3 and the central tracking system for τ -type 1.

In the $e\tau_h$ and $\mu\tau_h$ channels, an isolated lepton (e, μ) with transverse momentum above 15 GeV and an isolated hadronic tau with transverse momentum above 16.5 GeV (22 GeV for τ -type 3) are required. The pseudorapidity $|\eta|$ is less than 2 for muons and hadronic taus and 2.5 for electrons. In addition to the background from $Z/\gamma^* \rightarrow \tau^+\tau^-$ production, a $W(\rightarrow \ell\nu) + \text{jet}$ event can be misiden-

TABLE I. Expected number of events for backgrounds, number of events observed in the data, and efficiency for a signal with $M_\phi = 160$ GeV for the three channels. The uncertainties are statistical.

Channel	$e\tau_h$	$\mu\tau_h$	$e\mu$
$Z/\gamma^* \rightarrow \tau^+\tau^-$	581 ± 5	1130 ± 7	212 ± 3
Multijet	332 ± 20	86 ± 4	29 ± 1
$W \rightarrow e\nu, \mu\nu, \tau\nu$	42 ± 5	32 ± 4	9 ± 2
$Z/\gamma^* \rightarrow e^+e^-, \mu^+\mu^-$	31 ± 2	19 ± 1	12 ± 1
Diboson + $t\bar{t}$	3.0 ± 0.1	7.0 ± 0.4	6.1 ± 0.1
Total expected	989 ± 23	1274 ± 9	269 ± 3
Data	1034	1231	274
Efficiency (%)	1.04 ± 0.03	1.46 ± 0.04	0.57 ± 0.03

tified as a high-mass di-tau event if the jet is misidentified as a hadronic tau decay. The transverse mass, $M_T^{e/\mu} = [2p_T^{e/\mu} \cancel{E}_T (1 - \cos\Delta\varphi)]^{1/2}$, is required to be less than 40 GeV for the $\mu\tau_h$ and 50 GeV for the $e\tau_h$ channel. Here, $\Delta\varphi$ is the azimuthal angle between the lepton and \cancel{E}_T . In addition, a selection is made in the $\Delta\varphi(e/\mu, \cancel{E}_T) - \Delta\varphi(\tau, \cancel{E}_T)$ plane, such that $\Delta\varphi(e/\mu, \cancel{E}_T) < 3.5 - \Delta\varphi(\tau, \cancel{E}_T)$ if $\Delta\varphi(\tau, \cancel{E}_T) < 2.9$ or $\Delta\varphi(e/\mu, \cancel{E}_T) < 0.6$ otherwise. This selection removes events where the missing transverse energy is in the hemisphere opposite to the muon and the tau candidate. Because of the larger multijet background in the $e\tau_h$ channel the azimuthal angle between the electron and tau, $\Delta\varphi(e, \tau)$, is required to be greater than 1.6.

The $e\tau_h$ channel has a significant background from $Z/\gamma^* \rightarrow e^+e^-$ production, where an electron is misreconstructed as a hadronic tau candidate. To remove these events, the hadronic tau candidates in the $e\tau_h$ channel are required to be outside of the region $1.05 < |\eta| < 1.55$, where there is limited EM calorimeter coverage and are required to have less than 90% of their energy deposited in the EM calorimeter. Finally, τ -type 2 candidates are re-

quired to have $NN_e > 0.8$, which rejects 92% of the $Z/\gamma^* \rightarrow e^+e^-$ events, while retaining 83% of the $Z/\gamma^* \rightarrow \tau^+\tau^-$ events.

We select one muon with $p_T > 10$ GeV and one electron with $p_T > 12$ GeV in the $e\mu$ channel. Multijet and W boson production are suppressed by requiring the invariant mass of the electron-muon pair to be above 20 GeV and $\cancel{E}_T + p_T^e + p_T^\mu > 65$ GeV. Background from $W + \text{jet}$ events can be reduced using the transverse mass by requiring that either $M_T^e < 10$ GeV or $M_T^\mu < 10$ GeV. Furthermore, the minimum angle between the leptons and the \cancel{E}_T vector, $\min[\Delta\varphi(e, \cancel{E}_T), \Delta\varphi(\mu, \cancel{E}_T)]$, has to be smaller than 0.3. Contributions from $t\bar{t}$ background are suppressed by rejecting events where the scalar sum of the transverse momenta of all jets in the event is greater than 70 GeV.

The number of events observed in the data and expected from the various SM processes show good agreement (Table I). The M_{vis} distribution is shown in Fig. 1. The number of background and signal events depend on numerous measurements that introduce a systematic uncertainty: integrated luminosity (6.1%), trigger efficiency (3%–4%), lepton identification and reconstruction efficiencies (2%–10%), jet and tau energy calibration (2%–3%), PDF uncertainty (4%), the uncertainty on the Z/γ^* production cross section (5%), normalization of the W boson background (6%–15%), and modeling of multijet background (4%–40%). All except the last one are correlated among the three final states. Most of the uncertainties affect only the overall acceptance for the signal and backgrounds. However, uncertainties on the energy scale and electron trigger efficiencies modify the shape of the visible mass distribution. These uncertainties are therefore parametrized as a function of M_{vis} .

We extract upper limits on the production cross section times branching ratio as a function of Higgs boson mass M_ϕ . In order to maximize the sensitivity (median expected limit), the event samples of the $e\tau_h$ and $\mu\tau_h$ channels are

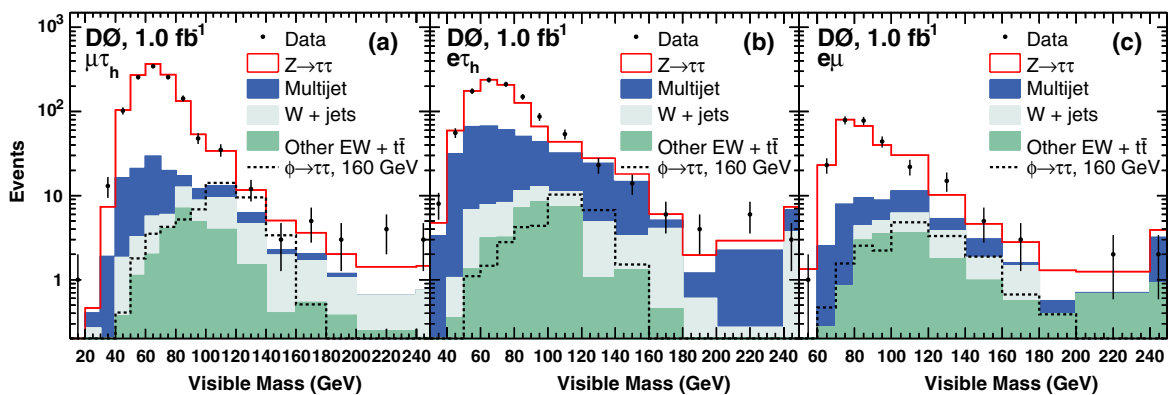


FIG. 1 (color online). The distribution of the visible mass M_{vis} for (a) $\mu\tau_h$, (b) $e\tau_h$, and (c) $e\mu$ channels compared to the sum of the expected backgrounds after all selections. The Higgs boson signal is normalized to a cross section of 3 pb. The highest bin includes the overflow.

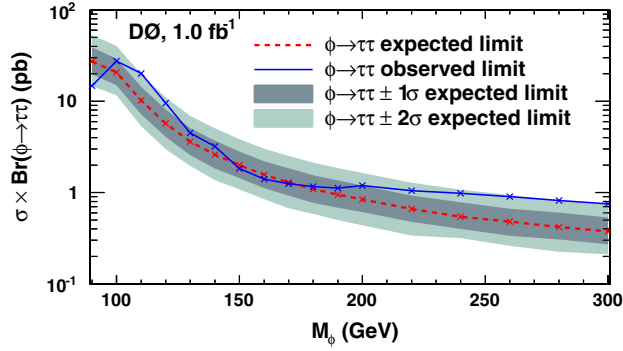


FIG. 2 (color online). Expected and observed 95% C.L. upper limits on the cross section times branching ratio for $\phi \rightarrow \tau^+ \tau^-$ production as a function of M_ϕ assuming the SM width of the Higgs boson. The $\pm 1, 2$ standard deviation bands on the expected limit are also shown.

separated by τ -type to exploit the different signal-to-background ratios. Furthermore the differences in shape between signal and background are exploited by using the full M_{vis} spectrum in the limit calculation (Fig. 1). The limits are calculated by utilizing a likelihood-fitter [13] that uses a log-likelihood ratio test statistic method. The confidence level C.L._s is defined as $\text{C.L.}_s = \text{C.L.}_{s+b}/\text{C.L.}_b$, where C.L._{s+b} and C.L._b are the confidence levels in the signal-plus-background and background-only hypotheses, respectively. The expected and observed limits are calculated by scaling the signal until $1 - \text{C.L.}_s$ reaches 0.95. The resulting cross section limits are shown in Fig. 2. The difference between the observed and expected limits at high masses is slightly above 2 standard deviations. It is mainly caused by a data excess in the $\mu\tau_h$ channel above M_{vis} of 160 GeV. A large number of kinematic distributions were studied for this sample and the data are consistent with both background and signal shapes. Because of the M_{vis} resolution these events affect the limit over a wide range of masses.

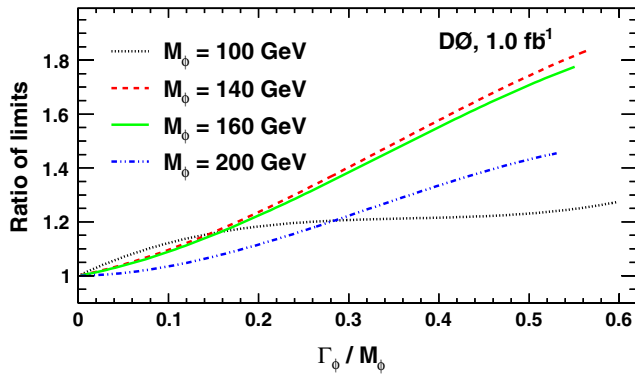


FIG. 3 (color online). Ratio of expected cross section limits using a Higgs boson with non-SM width to those calculated with a Higgs boson with SM width, as a function of Γ_ϕ/M_ϕ .

The limits in Fig. 2 assume a Higgs boson with SM width, which is negligible compared to the experimental resolution on M_{vis} . In models such as the MSSM the Higgs boson width can become substantially larger than the value in the SM. This was simulated by multiplying a relativistic Breit-Wigner (BW) function with the cross section from FEYNHIGGS [14] for masses $M > 80$ GeV to obtain the differential cross section for a wide Higgs boson as a function of mass:

$$\frac{d\sigma}{dM} = \sigma(M, \tan\beta, \Gamma_\phi = 0) \times \text{BW}(M, M_\phi, \Gamma_\phi). \quad (1)$$

This differential cross section was used to build a signal template of the M_{vis} distribution for a Higgs boson of mass M_ϕ and width Γ_ϕ . The limit calculation procedure was then repeated with templates corresponding to various values of Γ_ϕ . The ratio of the expected cross section limit for a wide Higgs boson to the limit for a Higgs boson with SM width as a function of Γ_ϕ/M_ϕ is shown in Fig. 3. This result can be used to correct the cross section limit for a Higgs boson with SM width (Fig. 2) for a non-SM width in a model independent way.

In the MSSM, the masses and couplings of the Higgs bosons depend, in addition to $\tan\beta$ and M_A , on the MSSM parameters through radiative corrections. In a constrained model, where unification of the SU(2) and U(1) gaugino masses is assumed, the most relevant parameters are the mixing parameter X_t , the Higgs mass parameter μ , the gaugino mass term M_2 , the gluino mass m_g , and a common scalar mass M_{SUSY} . Limits on $\tan\beta$ as a function of M_A are derived for two scenarios assuming a CP -conserving Higgs sector [15]: the m_h^{max} scenario [16] and the no-mixing scenario [17] with $\mu = +0.2$ TeV. The $\mu < 0$ case is not considered as it is currently disfavored [18]. The production cross sections, widths, and branching ratios for the Higgs bosons are calculated over the mass range from 90 GeV to 300 GeV using the FEYNHIGGS program [14]. In these scenarios $\Gamma_A/M_A < 0.1$ for $M_A < 200$ GeV. The effect of the Higgs boson width is therefore small. For large

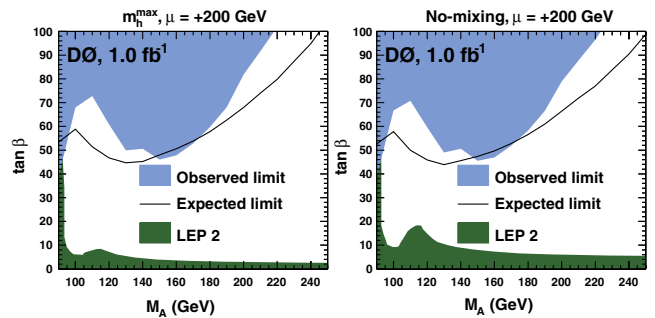


FIG. 4 (color online). Region in the $(M_A, \tan\beta)$ plane that is excluded at 95% C.L. for the m_h^{max} and the no-mixing scenario ($m_t = 172.6$ GeV [19]). Also shown is the excluded region from LEP [2].

$\tan\beta$, the A boson is nearly degenerate in mass with either the h or the H boson, and their production cross sections ($gg \rightarrow \phi$, $b\bar{b} \rightarrow \phi$) are added.

Figure 4 shows the results interpreted in the MSSM scenarios considered in the Letter. We reach a sensitivity of around $\tan\beta = 50$ for M_A below 180 GeV. The result represents the most stringent limit on the production of neutral MSSM Higgs bosons at hadron colliders.

We thank the staffs at Fermilab and collaborating institutions, and acknowledge support from the DOE and NSF (USA); CEA and CNRS/IN2P3 (France); FASI, Rosatom, and RFBR (Russia); CNPq, FAPERJ, FAPESP, and FUNDUNESP (Brazil); DAE and DST (India); Colciencias (Colombia); CONACyT (Mexico); KRF and KOSEF (Korea); CONICET and UBACyT (Argentina); FOM (The Netherlands); STFC (United Kingdom); MSMT and GACR (Czech Republic); CRC Program, CFI, NSERC, and WestGrid Project (Canada); BMBF and DFG (Germany); SFI (Ireland); the Swedish Research Council (Sweden); CAS and CNSF (China); and the Alexander von Humboldt Foundation.

*Visitor from Augustana College, Sioux Falls, SD, USA.

†Visitor from The University of Liverpool, Liverpool, UK.

‡Visitor from ICN-UNAM, Mexico City, Mexico.

§Visitor from II. Physikalisches Institut, Georg-August-University, Göttingen, Germany.

||Visitor from Helsinki Institute of Physics, Helsinki, Finland.

¶Visitor from Universität Zürich, Zürich, Switzerland.

**Deceased.

[1] H. P. Nilles, Phys. Rep. **110**, 1 (1984); H. E. Haber and G. L. Kane, Phys. Rep. **117**, 75 (1985).

- [2] S. Schael *et al.* (The ALEPH, DELPHI, L3, and OPAL Collaborations), Eur. Phys. J. C **47**, 547 (2006).
- [3] V. Abazov *et al.* (D0 Collaboration), Phys. Rev. Lett. **95**, 151801 (2005).
- [4] A. Abulencia *et al.* (CDF Collaboration), Phys. Rev. Lett. **96**, 011802 (2006).
- [5] V. Abazov *et al.* (D0 Collaboration), Phys. Rev. Lett. **97**, 121802 (2006).
- [6] T. Andeen *et al.*, Report No. FERMILAB-TM-2365 (2007).
- [7] V. Abazov *et al.* (D0 Collaboration), Nucl. Instrum. Methods Phys. Res., Sect. A **565**, 463 (2006).
- [8] T. Sjöstrand *et al.*, Comput. Phys. Commun. **135**, 238 (2001).
- [9] R. Brun and F. Carminati, CERN Program Library Long Writeup W5013 (1993).
- [10] J. Pumplin *et al.*, J. High Energy Phys. 07 (2002) 012.
- [11] V. M. Abazov *et al.* (D0 Collaboration), Phys. Rev. Lett. **100**, 241803 (2008).
- [12] V. Abazov *et al.* (D0 Collaboration), Phys. Rev. D **71**, 072004 (2005); **77**, 039901 (2008).
- [13] W. Fisher, Report No. FERMILAB-TM-2386-E (2007).
- [14] S. Heinemeyer, W. Hollik, and G. Weiglein, Eur. Phys. J. C **9**, 343 (1999); Comput. Phys. Commun. **124**, 76 (2000); G. Degrandi *et al.*, Eur. Phys. J. C **28**, 133 (2003); M. Frank *et al.*, J. High Energy Phys. 02 (2007) 047; FEYNHIGGS program: <http://www.feynhiggs.de>.
- [15] M. S. Carena, S. Heinemeyer, C. E. M. Wagner, and G. Weiglein, Eur. Phys. J. C **26**, 601 (2003).
- [16] $M_{\text{SUSY}} = 1$ TeV, $X_t = 2$ TeV, $M_2 = 0.2$ TeV, $\mu = +0.2$ TeV, and $m_g = 0.8$ TeV.
- [17] $M_{\text{SUSY}} = 2$ TeV, $X_t = 0$ TeV, $M_2 = 0.2$ TeV, $\mu = +0.2$ TeV, and $m_g = 1.6$ TeV.
- [18] J. R. Ellis, S. Heinemeyer, K. A. Olive, A. M. Weber, and G. Weiglein, J. High Energy Phys. 08 (2007) 083.
- [19] The Tevatron Electroweak Working Group (CDF and D0 Collaborations), arXiv:0803.1683.